Hindawi
Advances in Civil Engineering
Volume 2021, Article ID 9134889, 11 pages
https://doi.org/10.1155/2021/9134889

Research Article

Experimental Research on Thermomechanical Properties of Thermal Energy Storage Cement Mortar Incorporated with Phase-Change Material

Kunyang Yu,[1,2] **Yong Huang**,[1] **Bo Jin**,[1] **and Yushi Liu**[1,2]

[1]*Key Laboratory of Earthquake Engineering and Engineering Vibration, Institute of Engineering Mechanics, China Earthquake Administration, Harbin, China*
[2]*School of Civil Engineering, Harbin Institute of Technology, Harbin 150090, China*

Correspondence should be addressed to Bo Jin; jinbo@iem.ac.cn and Yushi Liu; liuyushi@hit.edu.cn

Received 13 April 2021; Revised 8 July 2021; Accepted 3 August 2021; Published 11 August 2021

Academic Editor: Filippo Ubertini

In the current work, the thermal energy storage cement mortars were prepared by physical mixing between cement mortar and form-stable hydrated salt based on disodium hydrogen phosphate dodecahydrate/carbon nanofiber-expanded graphite (DSP/CNF-EG). The DSP/CNF-EG was incorporated into cement mortar through replacing standard sand of 5 wt%, 10 wt%, and 15 wt%. The pore structure results obtained from the mercury intrusion porosimeter (MIP) demonstrated that the incorporation of DSP/CNF-EG form-stable hydrated salt PCM can cause the increased porosity of the cement mortar. The mechanical strengths of the thermal energy storage cement mortars were decreased with increasing DSP/CNF-EG incorporation amount, and they still meet the strengths of the building envelope. Moreover, dynamic mechanical analysis (DMA) results suggested that the damping properties of the thermal energy storage cement mortar were enhanced by incorporating DSP/CNF-EG, which were related to the porosity and the internal friction action. In addition, the thermal conductivity and the specific heat capacity results confirmed that the introduction of DSP/CNF-EG can endow cement mortar with excellent thermal energy storage capacity. The thermal performance test further indicated that the thermal energy storage cement mortar showed good endothermic and exothermic characteristics, and it played a prominent role in weakening the indoor temperature peak.

1. Introduction

With the continuous consumption of fossil fuels, the issue of energy shortage is becoming increasingly serious. In particular, energy applied in buildings accounts for more than 30% of the global total energy consumption [1]. Therein, the energy consumption of thermal form is dominant. For this reason, thermal energy storage building materials have been developed by incorporating phase-change materials (PCMs) into building materials. [2, 3]. The building materials incorporating PCMs can realize the building energy saving relied on the feature of PCMs absorbing and releasing heat during the phase transition. Moreover, building thermal fluctuation can be mitigated based on the latent heat storage capacity of PCMs as well [4, 5]. Therefore, building energy saving and indoor thermal comfort are achieved by the incorporation of PCMs into building materials [6, 7].

The typical building materials include concrete [8–13], cement mortars [14, 15], and gypsum [16, 17]. Among various building materials, cement mortars have been widely used in walls and are highly suitable for the incorporation of PCMs due to the larger area occupied in doors. The incorporation approaches of PCMs into the cement mortar mainly include three kinds: one is that PCMs are directly immersed into the cement mortar [18], the second is that PCMs are encapsulated and then incorporated into cement mortar [19], and the third is that macroencapsulated PCMs [20] or composite PCMs [21] are integrated into the cement mortar in the form of layered panels. Although the direct immersion method is simple and of low cost, PCMs are easy

to seep from cement mortar undergoing several heating-cooling cycles. This is unacceptable due to the large loss of heat storage capacity. As for layered panels containing PCMs, the layered structure leads to the increase in wall thickness, inevitably occupying a lot of building space. The encapsulated PCMs (also known as form-stable PCMs) can effectively avoid the leakage of PCMs. In recent years, a large number of thermal energy cement mortars containing form-stable PCM (FSPCM) were developed. For example, Sang et al. [22] prepared a kind of thermal energy storage cement-based mortar with good thermal performance by incorporating 25.9 wt% form-stable organic PCM. He et al. [23] synthetized a fatty acid/expanded perlite FSPCM, and then the FSPCM was added into the cement mortar to form the phase-change mortar composite. The results indicated that the air temperature of the simulated indoor box was well controlled using this composite. Sun and Wang [24] adopted epoxy resin to coat the FSPCM with paraffin core material and expanded perlite support and then explored the influence of the FSPCM incorporation amount on the mechanical properties of the prepared phase-change mortar. It turned out that the compressive and flexural strengths of the phase-change mortar were decreased by increasing the FSPCM content. Ramakrishnan et al. [25] used paraffin/hydrophobic expanded perlite FSPCM to replace 80 vol.% quartz sand to prepare the thermal energy storage mortar. It was found that the compressive strength of the mortar cured by 28 days was decreased by 66.7% compared with that of the control mortar. Zhang et al. [26] investigated the evolution of compressive strength of cement mortar containing octadecane/expanded graphite FSPCM. The result suggested that the compressive strength of the mortar showed a significant deterioration from 23.7 MPa to 10.5 MPa when octadecane/expanded graphite FSPCM reached to 2.5% incorporating amount. Xu et al. [27] developed a lightweight mortar with thermal energy storage capacity using paraffin/expanded vermiculite FSPCM to completely replace the river sand. The 28-day compressive strength of the lightweight mortar was 18.1 MPa, which was decreased by 56.5% compared with that of the mortar with river sand.

Based on the above research situation, most of research studies only adopted form-stable organic PCMs to fabricate the thermal energy storage mortar. However, the features of higher cost and lower latent heat of organic PCMs severely limit their applications in buildings. In addition, the universal flammability of organic PCMs also rises building fire risk [28]. Inorganic hydrated salt PCMs have been attracting increasing attention for thermal energy storage due to the advantages of low cost, high latent heat, nonflammability, etc. [29, 30]. Moreover, the phase-change temperature of most inorganic hydrated salt PCMs is closer to the temperature range of indoor thermal comfort compared to the organic PCMs [29]. Hence, form-stable inorganic PCMs have a promising application in terms of preparing thermal energy storage mortar.

In addition, the mechanical properties of cement mortar containing form-stable PCMs should be inspected as well since its good mechanical properties can ensure the favorable workability and serviceability. Nevertheless, the current research studies have been only focused on the static mechanical properties such as compressive strength and flexural strength of the cement mortar incorporating form-stable PCM. The results from the reported works indicated that the static mechanical properties of the cement mortar incorporating form-stable PCM were significantly deteriorated. Moreover, the degradation level of static mechanics increases with the increase of the percentage of form-stable phase-change materials [31]. The reasons could be explained by the poor compatibility between the form-stable PCM and cement matrix and the soft matter nature of form-stable PCMs [32]. These two reasons lead to the increase of porosity and the decrease of local elastic modulus of cement mortar. Although some efforts have been made to study the incorporation of form-stable PCMs on the static mechanical properties of cement mortar, to date, the research on the dynamic mechanical properties for cement mortar incorporating form-stable PCMs is hardly found in the literature studies.

Notably, the introduction of form-stable PCMs into mortar usually results in the increased porosity and the decreased elastic modulus of mortar. However, the dynamic mechanical properties of mortar are greatly affected by the changes in the porosity and the elastic modulus. In particular, the energy dissipation for cement mortar under dynamic load will be enhanced through the increase of porosity and the decrease of elastic modulus [33]. Therefore, it can be expected that the ability of cement mortar to resist some dynamic actions may be enhanced by the incorporation of form-stable PCMs.

In our group's previous work, a novel disodium hydrogen phosphate dodecahydrate/carbon nanofiber-expanded graphite (DSP/CNF-EG) hybrid composite with a melting temperature of 33.7°C and latent heat of 208.9 J/g was developed as a form-stable hydrated salt PCM for building energy saving. In this work, we used DSP/CNF-EG to prepare a novel thermal energy storage cement mortar based on the mechanical blending between cement mortar and DSP/CNF-EG. The compressive strength, flexural strength, pore structure, thermal conductivity, specific heat capacity, and thermal energy storage performance of the cement mortar containing DSP/CNF-EG were investigated. In addition, the damping property of the prepared thermal energy storage cement mortar was tested to evaluate its dynamic mechanical performance.

2. Materials and Methods

2.1. Raw Materials. The PO 42.5 ordinary Portland cement was supplied by Yatai Co., Ltd., and the physical properties are shown in Table 1. The standard sand was obtained from Sinoma Co., Ltd. Based on the synthetic method described by our previous work [34], the disodium hydrogen phosphate dodecahydrate/carbon nanofiber-expanded graphite (DSP/CNF-EG) form-stable hydrated salt phase-change material was prepared, and the average particle size of DSP/CNF-EG used in this work was consistent with that of standard sand (≤2 mm). The specific preparation process of DSP/CNF-EG was as follows: first, 50 g disodium hydrogen

Table 1: Physical properties of the PO 42.5 ordinary Portland cement.

Setting time (min)		Compressive strength (MPa)		Flexural strength (MPa)	
Initial setting	Final setting	3 d	28 d	3 d	28 d
185	239	16.9	46.6	4.8	7.5

phosphate dodecahydrate (DSP) was poured into a beaker kept in the thermostatic water bath at 65°C and melted to form the clear and transparent solution; afterwards, 0.75 g carbon nanofiber (CNF) was added into the DSP solution, followed by stirring it for 2 hours at 1600 rpm; then, 1 g expanded graphite (EG) was further added into the DSP/CNF suspension, and the mixture was continued to stir for 6 hours at 65°C; lastly, DSP/CNF-EG was obtained via the suction filtration method.

2.2. Preparation and Characterization of Thermal Energy Storage Cement Mortar Containing Form-Stable Hydrated Salt PCM

2.2.1. Mix Proportion. The mix proportion of control cement mortar (CM) is shown in Table 2. Three thermal energy storage cement mortar (TESCM) samples were fabricated by incorporating DSP/CNF-EG into the cement mortar using physical mixing. The specific process is as follows: firstly, a certain amount of DSP/CNF-EG and sand were fully mixed in an agitator for 3 min at 125 rpm; afterwards, cement and water were poured into the agitator and further stirred for 3 min; finally, the thermal energy storage mortar samples were casted in mould. Figure 1 presents the schematic illustration of fabricating thermal energy storage cement mortar containing DSP/CNF-EG by physical blending. DSP/CNF-EG was introduced into CM through partially replacing standard sand. The replacement levels of DSP/CNF-EG were 0, 5 wt%, 10 wt%, and 15 wt%, respectively. The CMs with different replacement levels of DSP/CNF-EG were named as DSP/CNF-EG/CM-3.3, DSP/CNF-EG/CM-6.7, and DSP/CNF-EG/CM-10 based on the mass ratio of DSP/CNF-EG to DSP/CNF-EG/CM.

2.2.2. Compressive Strength and Flexural Strength Test. The CM and DSP/CNF-EG/CM were casted into 40 mm × 40 mm × 160 mm moulds followed by curing in the condition of 20 ± 2°C and relative humidity (RH) ≥ 99% for 28 days. 28-day compressive strengths and 28-day flexural strengths of CM and DSP/CNF-EG/CM samples were tested based on ISO 679:1989 and GB/T 17671-1999. For each sample, the tests were repeated 3 times, and the strength value of each data point was represented as mean ± standard deviation.

2.2.3. Pore Structure Analysis. The pore structure distribution of CM and DSP/CNF-EG/CM samples was measured by an IV 9510 mercury intrusion porosimeter (MIP), and the pressure was set within the range of 0–60,000 psi. The samples were cut into about 4-5 mm particles.

2.2.4. Thermal Conductivity and Specific Heat Capacity Measurement. The thermal conductivity and specific heat capacity of CM and DSP/CNF-EG/CM samples were measured by using a laser thermal conductivity measuring instrument (NETZSCH, Newsletter-LFA467). The size of the samples was $9.5 \times 9.5 \times 2.0\,mm^3$.

2.2.5. Thermal Performance Test. The self-designed heating setup (Figure 2) was carried out for evaluating the thermal performance of CM and DSP/CNF-EG/CM samples. As shown in Figure 2, the self-designed heating setup mainly contained a 100 W infrared lamp mounted on the top bracket, a polystyrene test box, and the multichannel temperature measuring system. A rectangular opening was cut at the upper surface center of the test box to place CM and DSP/CNF-EG/CM samples with the size of $200 \times 150 \times 20\,mm^3$. Two thermocouples were, respectively, fixed on the lower surface of the samples and the center of the test box to record the temperature change. The temperature data were recorded every 5 min. The infrared lamp was used as the heating source to heat the samples for 80 min. Subsequently, the infrared lamp was turned off, and the sample was naturally cooled for 120 min.

2.2.6. Damping Properties' Test. The damping properties' test procedure of the samples was provided by Yu et al. [35]. Dynamic mechanical analysis (DMA Q800, TA Instruments) was used to measure the damping properties of CM and DSP/CNF-EG/CM samples with the size of 40 mm × 10 mm × 2 mm. The samples were tested in the three-point bending mode with a span of 50 mm at 20°C. The sine waves with a frequency of 0.2 Hz were collected, and the displacement amplitude was 10 μm. Three parameters of loss tangent (η), storage modulus (E′), and loss modulus (E″) relating to the damping properties were obtained.

3. Results and Discussion

3.1. Pore Structure Analysis of DSP/CNF-EG/CM. The pore structure analysis results of CM and DSP/CNF-EG/CM samples cured for 28 days are shown in Figure 3. Figure 3(a) presents the pore diameter distribution of CM, DSP/CNF-EG/CM-3.3, DSP/CNF-EG/CM-6.7, and DSP/CNF-EG/CM-10. It can be found that the pores of DSP/CNF-EG/CM in the range of 100 nm–100 μm significantly increased with the increase of the replacement amount of DSP/CNF-EG form-stable hydrated salt PCM. Figure 3(b) shows the relationship between cumulative mercury pore volume and pore diameter of CM, DSP/CNF-EG/CM-3.3, DSP/CNF-EG/CM-6.7, and DSP/CNF-EG/CM-10. It can be seen that the curves of DSP/CNF-EG/CM samples deviated the direction of larger pore size. Moreover, the deviation became more obvious as the incorporation of DSP/CNF-EG increased. In order to present the detailed difference in the

Table 2: Mix proportion of cement mortar.

Water/cement	Cement/standard sand	DSP/CNF-EG replacing sand amount	Mass ratio of DSP/CNF-EG to DSP/CNF-EG/CM
1 : 2	1 : 3	0	0
		5 wt%	3.3 wt%
		10 wt%	6.7 wt%
		15 wt%	10.0 wt%

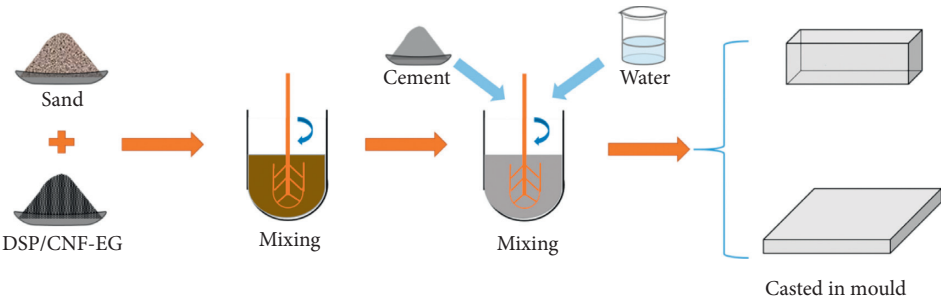

Figure 1: Schematic illustration of fabricating thermal energy storage cement mortar containing DSP/CNF-EG by physical blending.

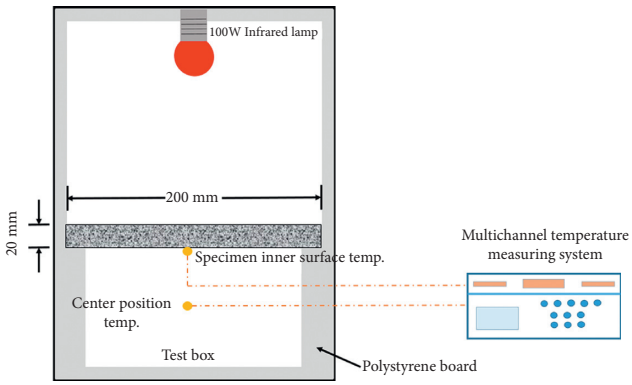

Figure 2: Schematic illustration of the self-designed heating setup.

pore structure of CM and DSP/CNF-EG/CM samples, the total porosity and the proportion of pores greater than 100 nm in the total pore are reorganized in Figures 3(c) and 3(d), respectively. As shown in Figure 3(c), the total porosities of DSP/CNF-EG/CM samples were much higher than those of CM (12.18%). Moreover, with the increase of DSP/CNF-EG incorporation amount, the total porosities of DSP/CNF-EG/CM samples also increased gradually. Therein, DSP/CNF-EG/CM-10 showed the highest total porosity of 14.74%. The pores with the size of larger than 100 nm need to be emphatically investigated because they had adverse effects on compressive and flexural strengths of mortars [36, 37]. It was notable from Figure 3(d) that the percentages of pores with the size of larger than 100 nm were gradually increased from CM of 51.1% to DSP/CNF-EG/CM-10 of 63.7% by the elevation of DSP/CNF-EG incorporation amount.

The increases of total porosity and pores with the size of larger than 100 nm can be attributed to the inferior compatibility between the cement matrix and DSP/CNF-EG form-stable hydrated salt PCM. To be specific, the main support of DSP/CNF-EG was expanded graphite (EG), and its surface property was hydrophobic. This made it difficult to retain water around DSP/CNF-EG. It was well known that the hardened cement was formed by the hydration reaction between cement clinker and water. Therefore, less hardened cement was formed around DSP/CNF-EG particles compared with that of control CM, resulting in the increase of porosity and formation of larger size pores.

3.2. Compressive Strength and Flexural Strength of DSP/CNF-EG/CM. The compressive strengths and flexural strengths of CM and DSP/CNF-EG/CM samples cured for 7 days and 28 days are displayed in Figure 4. As shown in Figure 4(a), the compressive strengths and flexural strengths of DSP/CNF-EG/CM samples cured for 7 days gradually decreased with increasing DSP/CNF-EG form-stable hydrated salt PCM. The 7-day compressive strengths were 29.3 ± 0.7 MPa, 20.2 ± 0.5 MPa, 14.7 ± 0.9 MPa, and 8.3 ± 0.4 MPa for CM, DSP/CNF-EG/CM-3.3, DSP/CNF-EG/CM-6.7, and DSP/CNF-EG/CM-10 samples. As for the 7-day flexural strengths, the values of CM, DSP/CNF-EG/CM-3.3, DSP/CNF-EG/CM-6.7, and DSP/CNF-EG/CM-10 samples were 7.1 ± 0.4 MPa, 4.5 ± 0.3 MPa, 3.9 ± 0.3 MPa, and 3.1 ± 0.5 MPa. Figures 4(c) and 4(d) show the compressive strengths and flexural strengths of CM and DSP/CNF-EG/CM samples cured for 28 days. With the prolongation of curing time, it can be seen that 28-day compressive and flexural strengths of each sample were increased compared with the 7-day compressive and flexural strengths of the samples. However, the downward trend of 28-day strengths of DSP/CNF-EG/CM samples was still unchanged with the incorporation of DSP/CNF-EG. To be specific, the 28-day compressive strengths of CM, DSP/CNF-EG/CM-3.3, DSP/CNF-EG/CM-6.7, and DSP/CNF-EG/CM-10 were 40.9 ± 1.3 MPa, 31.9 ± 0.8 MPa, 19.7 ± 1.6 MPa, and 12.5 ± 0.7 MPa, respectively. As for 28-day flexural strengths,

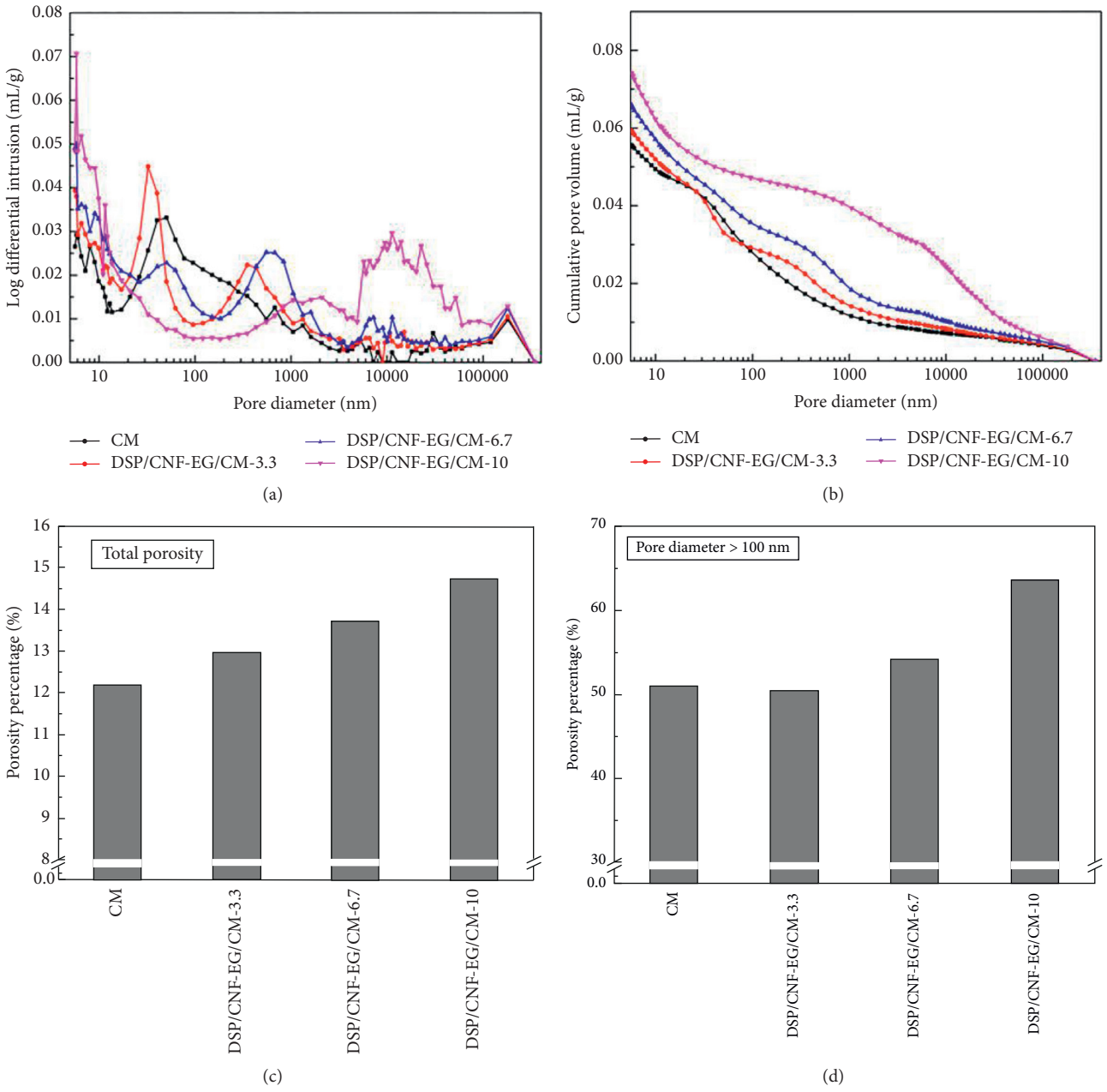

Figure 3: Pore structure analysis of CM, DSP/CNF-EG/CM-3.3, DSP/CNF-EG/CM-6.7, and DSP/CNF-EG/CM-10: (a) pore diameter distribution, (b) cumulative pore volume, (c) total porosity, and (d) the proportion of pores greater than 100 nm in the total pore.

the values were 7.4 ± 0.4 MPa, 5.3 ± 0.5 MPa, 4.5 ± 0.2 MPa, and 3.3 ± 0.1 MPa, respectively.

From the above results, the compressive strengths and flexural strengths of DSP/CNF-EG/CM decreased with increasing DSP/CNF-EG form-stable hydrated salt PCM incorporation. This was similar to most of thermal energy storage mortars containing form-stable PCMs reported in literature studies [14, 38]. The degradation of mechanical properties of DSP/CNF-EG/CM samples may be ascribed to the two reasons. On the one hand, the hydrophobicity of supporting materials EG and CNF of DSP/CNF-EG resulted in the formation of the loose interfacial transition zone between DSP/CNF-EG and cement matrix. This led to the increase of total porosity within DSP/CNF-EG/CM, which had been confirmed by the results of the pore structure as described in Section 3.1. Moreover, the pores with the size of larger than 100 nm were also increased. This had a great negative impact on the mechanical properties of mortars [36, 37]. On the other hand, sand played a skeleton role in mortar, which contributed to the mechanical properties of mortar. The composition of standard sand used in this study was natural quartz. The natural quartz had excellent strength performance. However, the CNF-EG hybrid structure in DSP/CNF-EG was porous and loose; thus, the strength of DSP/CNF-EG mainly came from DSP. Apparently, the mechanical strength of both crystalline DSP and molten DSP

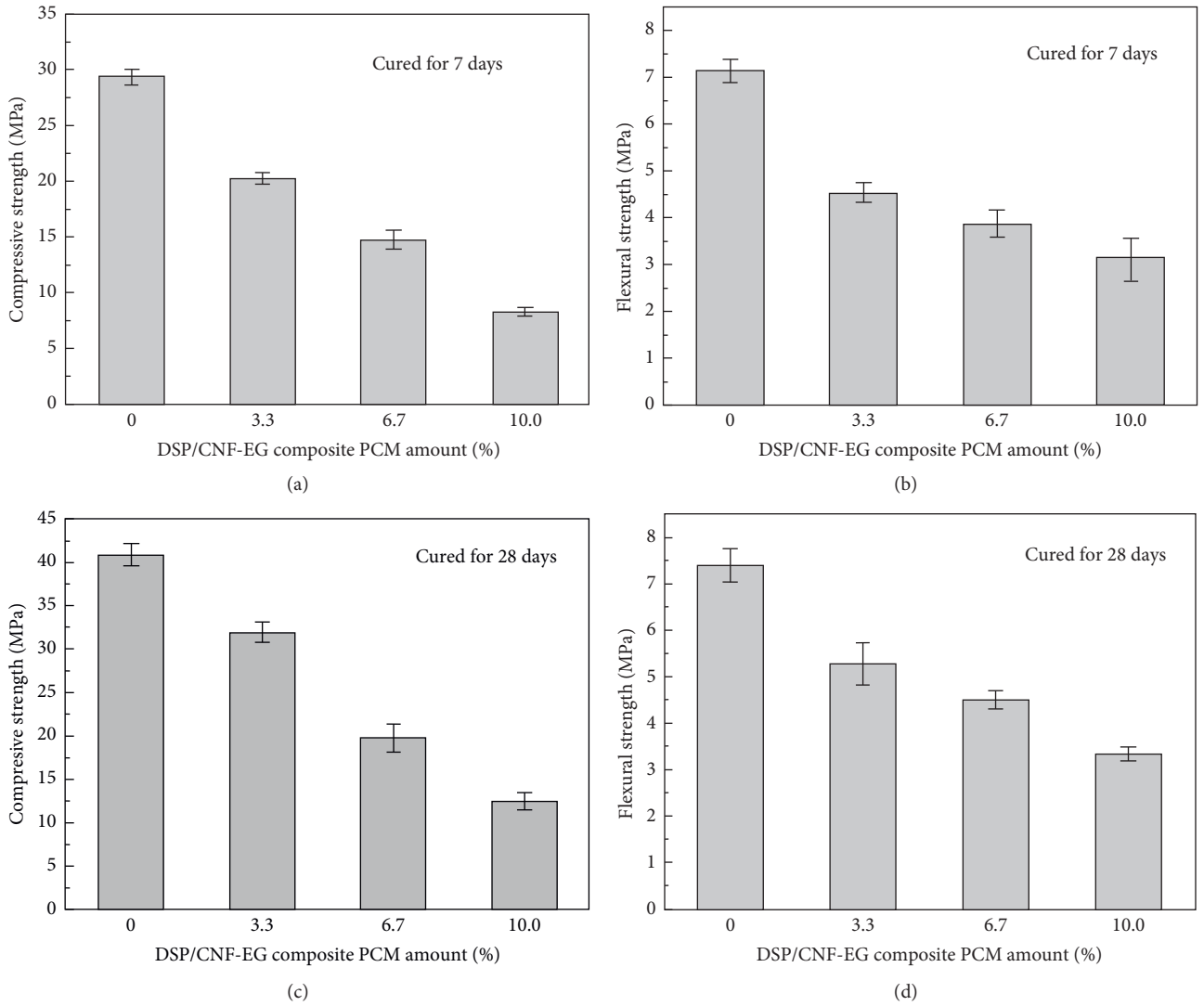

Figure 4: Compressive strength and flexural strength of CM and DSP/CNF-EG/CM samples with different curing periods: compressive strength cured for (a) 7 days and (c) 28 days and flexural strength cured for (b) 7 days and (d) 28 days.

was far less than that of natural quartz. Hence, the skeleton supporting function of DSP/CNF-EG form-stable PCM in the mortar was significantly weaker than that of sand. Although the mechanical properties of DSP/CNF-EG/CM decreased significantly, DSP/CNF-EG/CM-10 with the lowest compressive strength of 12.5 MPa still met the strength grade requirements for masonry mortar and plastering mortar based on the Chinese National Standard GB50574-2010. Hence, the prepared thermal energy storage cement mortar can be applied in the building envelope.

3.3. Damping Properties of DSP/CNF-EG/CM. The parameters reflecting damping properties of CM and DSP/CNF-EG/CM samples cured for 28 days are displayed in Figure 5. As shown in Figure 5(a), it can be seen that the storage modulus of DSP/CNF-EG/CM samples presented a downward trend with the increasing content of DSP/CNF-EG because of the weakening of bearing capacity. The maximum decrease range was from the control CM of 22.4 GPa to DSP/CNF-EG/CM-10 of 16.5 GPa. However, the loss modulus of the samples was increased with the gradual incorporation of DSP/CNF-EG. This phenomenon can be due to the fact that the enriched porosity of cement mortar led to the increase of energy dissipation [33]. In addition, the loose contact between DSP/CNF-EG and cement matrix could cause the interface friction action, also dissipating a lot of energy under the vibration load [39]. Based on the obtained storage modulus and loss modulus, the loss tangent of the samples can be calculated by using the following equation [40]:

$$\eta = \frac{E''}{E'} = 2\zeta, \tag{1}$$

where η is the loss tangent, E'' is the storage modulus, E' is the loss modulus, and ζ is the damping ratio of the samples. Therein, the parameter η can be used as the index to evaluate the damping of CM and DSP/CNF-EG/CM samples. Larger

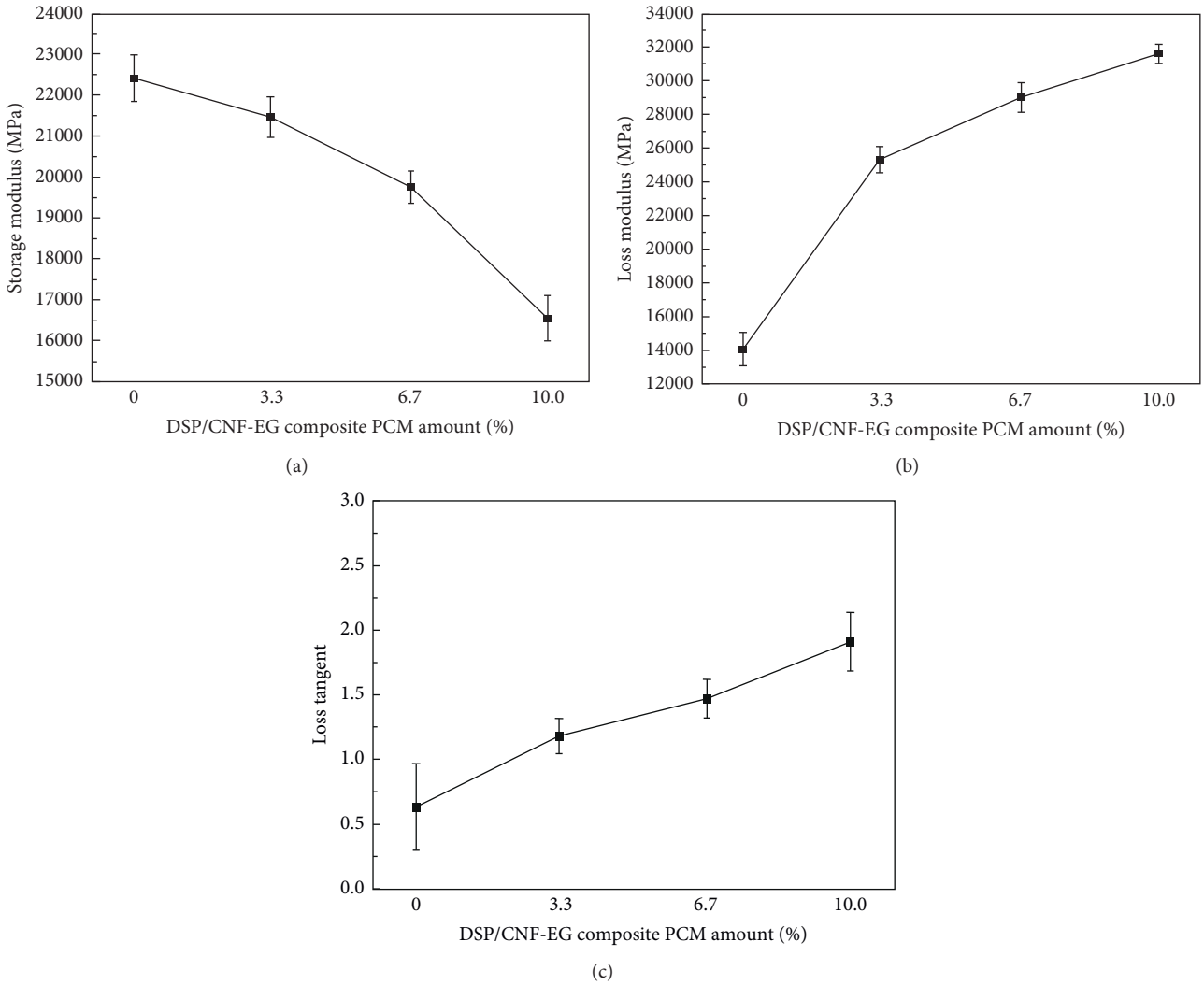

Figure 5: Damping properties of CM and DSP/CNF-EG/CM samples: (a) storage modulus, (b) loss modulus, and (c) loss tangent.

η means that the samples can weaken more vibration and dissipate more energy under the action of dynamic load, and vice versa [40].

As shown in Figure 5(c), the loss tangent values of CM, DSP/CNF-EG/CM-3.3, DSP/CNF-EG/CM-6.7, and DSP/CNF-EG/CM-10 were 0.63 ± 0.34, 1.18 ± 0.13, 1.47 ± 0.15, and 1.91 ± 0.23, respectively. Obviously, the addition of DSP/CNF-EG played a great positive role in enhancing the damping performance for DSP/CNF-EG/CM samples. This was profound because it enriches the functionality of thermal energy storage cement mortar containing form-stable PCM. This provided a novel insight into achieving the dual purpose of resisting dynamic load and improving heat storage capacity for cement mortar by the introduction of form-stable PCMs.

3.4. Thermal Conductivity and Specific Heat Capacity of DSP/CNF-EG/CM. Thermal conductivity and specific heat capacity of CM and DSP/CNF-EG/CM samples are shown in Figure 6. For each sample, the experiments were repeated 5 times, and the value of each data point was presented as the mean value ± standard deviation. As shown in Figure 6(a), the thermal conductivities of CM, DSP/CNF-EG/CM-3.3, DSP/CNF-EG/CM-6.7, and DSP/CNF-EG/CM-10 were 1.173 W/m·K, 0.934 W/m·K, 0.852 W/m·K, and 0.726 W/m·K, respectively. It can be found that the incorporation of DSP/CNF-EG form-stable hydrated salt caused the decreased thermal conductivity for cement mortar. DSP/CNF-EG/CM-10 had the lowest thermal conductivity, which is 38.1% lower than that of control CM. As for specific heat capacity, the results exhibited a contrary trend to the thermal conductivity. The specific heat capacity values of CM and DSP/CNF-EG/CM samples were 1.263 kJ/kg·K, 1.398 kJ/kg·K, 1.472 kJ/kg·K, and 1.621 kJ/kg·K, respectively. The highest specific heat capacity of DSP/CNF-EG/CM-10 was 28.3% higher than that of control CM. In many reported works [18, 26], the cement mortars containing form-stable PCMs showed reduced thermal conductivity and elevated specific heat capacity. This was due to the enhanced thermal energy storage capacity of the mortar samples by incorporation of DSP/CNF-EG. Therefore, the obtained results

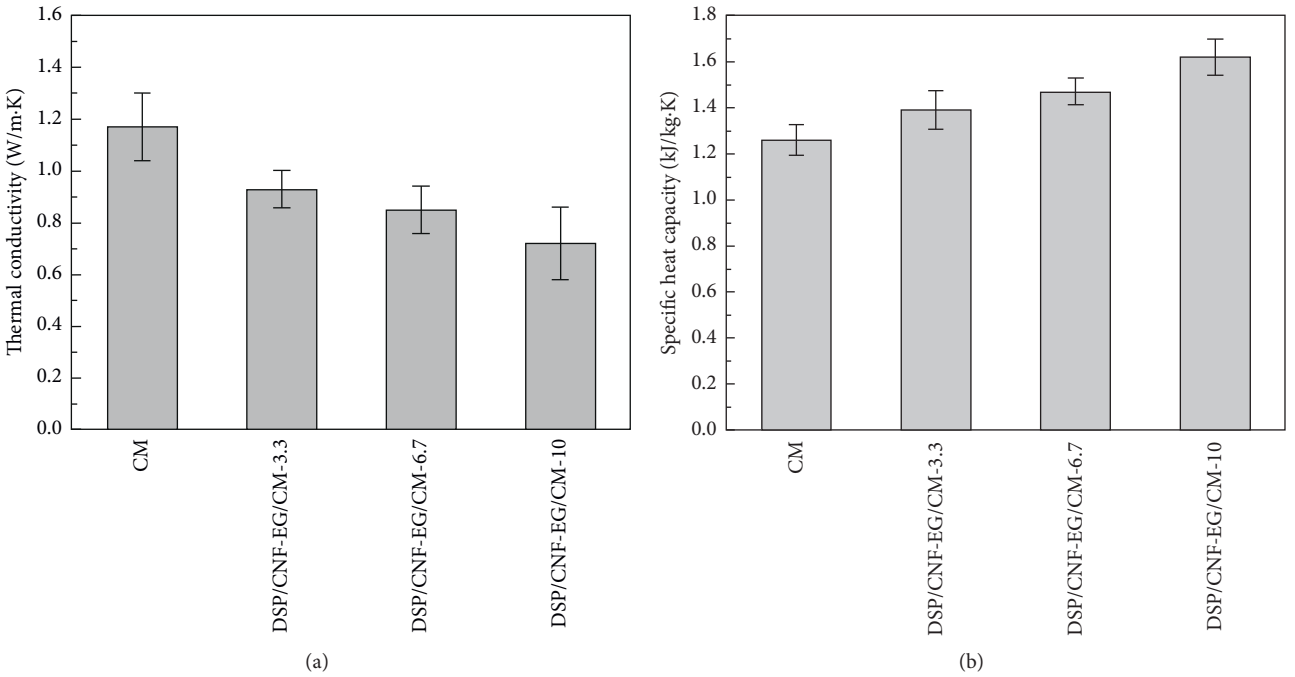

Figure 6: Thermal conductivity (a) and specific heat capacity (b) of CM and DSP/CNF-EG/CM samples.

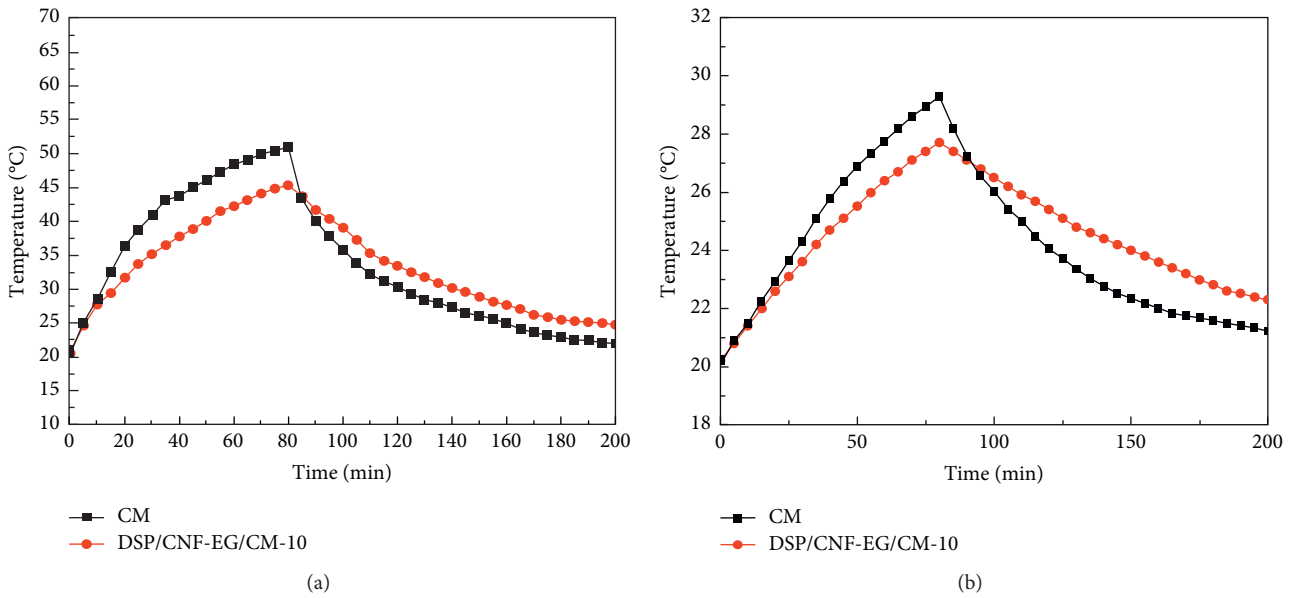

Figure 7: Thermal performance comparison between CM and DSP/CNF-EG/CM-10: (a) the temperature-time curves at the lower central surface of CM and DSP/CNF-EG/CM-10 specimens and (b) the temperature-time curves in the center position in the test box.

confirmed that the introduction of DSP/CNF-EG can endow cement mortar with excellent thermal energy storage capacity.

3.5. Thermal Performance Evaluation of DSP/CNF-EG/CM. The thermal performance comparison between CM and DSP/CNF-EG/CM-10 specimens is depicted in Figure 7. As shown in Figure 7(a), the temperature peak value of DSP/CNF-EG/CM-10 was much lower than that of the control CM. To be specific, the temperature peak values of CM and DSP/CNF-EG/CM-10 specimens were 51.1°C and 45.3°C, respectively, showing a temperature peak weakening of 5.8°C. This confirmed endothermic and exothermic features of DSP/CNF-EG/CM-10 during the heating and cooling process. Figure 7(b) shows the temperature-time curves at

the center position in the test box with, respectively, covering control CM and DSP/CNF-EG/CM-10 specimens. It can be found that their temperature curves were highly similar to those displayed in Figure 7(a). The temperature-time curve in the center position in the test box covering the DSP/CNF-EG/CM-10 specimen was gentle compared to that of control CM, showing an excellent temperature control performance. Moreover, the temperature peak for covering the DSP/CNF-EG/CM-10 specimen was significantly reduced by 1.6°C compared with that of control CM.

In the previous reports from literature studies, some researchers also fabricated the test box with one side replaced by the thermal energy storage building material specimen plate to evaluate the thermal energy storage performance. These reports indicated that the specimen plate with the thermal energy storage property can weaken the indoor temperature fluctuation. For example, Xu et al. [27] prepared a kind of lightweight thermal energy storage cement-based composite (LW-TESCC) by incorporating paraffin/expanded vermiculite form-stable PCM. The obtained result indicated that the temperature peak inside the test box equipped with the LW-TESCC plate was weakened by 2°C compared with that of the control specimen. Li et al. [41] measured the thermal energy storage cement mortar (TESCM) containing paraffin/expanded graphite form-stable PCM. The results indicated that the temperature peak in the test box fitted with the TESCM plate could be significantly reduced by 2.2°C, compared with that of the control CM plate. Fang et al. [42] found that the gypsum plate incorporating 20 wt% RT20/MMT phase-change composite could reduce the internal temperature peak of the test box by 5°C. In this study, although different test boxes are used, the prepared DSP/CNF-EG/CM-10 also showed the ability to weaken the temperature peak, reflecting the excellent indoor temperature control performance.

4. Conclusions

In summary, DSP/CNF-EG form-stable hydrated salt PCM was incorporated into cement mortar by physical mixing to fabricate thermal energy storage cement mortar. Based on the experiment results and the profound discussion, the following conclusions can be obtained:

(1) As the level of DSP/CNF-EG replacing sand increased, the pore size distributions of DSP/CNF-EG/CM samples were gradually shifted to the larger pore size, and the total porosity and the pores with the size of larger than 100 nm were also increased due to the inferior interface compatibility between DSP/CNF-EG and cement matrix.

(2) The compressive strength of DSP/CNF-EG/CM gradually decreased with the increasing content of DSP/CNF-EG. As the incorporation amount of DSP/CNF-EG reached to 10 wt%, DSP/CNF-EG/CM-10 presented the 28-day compressive strength of 12.5 MPa. The compressive strength could well meet the strength requirement applied in the building envelope.

(3) The introduction of DSP/CNF-EG played a positive role in enhancing the damping properties of DSP/CNF-EG/CM because enriched porosity and interface friction action of DSP/CNF-EG/CM significantly increased the energy dissipation under dynamic load. The loss tangent of DSP/CNF-EG/CM-10 was 1.91, showing 203.2% increase compared with that of control CM.

(4) The incorporation of DSP/CNF-EG resulted in the reduced thermal conductivity and elevated specific heat capacity of DSP/CNF-EG/CM. DSP/CNF-EG/CM-10 had the lowest thermal conductivity of 0.726 W/m·K and the highest specific heat capacity of 1.621 kJ/kg·K.

(5) The DSP/CNF-EG/CM-10 specimen plate was integrated into the upper side of the test box of the self-design heating setup to evaluate the thermal performance. The results illustrated that the thermal energy storage capacity of cement mortar was improved by the incorporation of DSP/CNF-EG form-stable hydrated salt PCM.

Overall, the introduction of DSP/CNF-EG form-stable hydrated salt PCM endowed cement mortar with good heat storage capacity. The formed thermal energy storage cement mortar can be used in building envelopes and to improve the relationship between supply and demand in terms of building thermal energy, thus achieving building energy saving.

Data Availability

The data used to support the findings of this study are available from the corresponding author upon request.

Conflicts of Interest

The authors declare that they have no conflicts of interest.

Acknowledgments

The financial support from the Scientific Research Fund of Institute of Engineering Mechanics, China Earthquake Administration (Grant no. 2020D09) for the current research is gratefully acknowledged.

References

[1] P. Sukontasukkul, P. Uthaichotirat, T. Sangpet et al., "Thermal properties of lightweight concrete incorporating high contents of phase change materials," *Construction and Building Materials*, vol. 207, pp. 431–439, 2019.

[2] Y. Liu, E. Xu, M. Xie, X. Gao, Y. Yang, and H. Deng, "Use of calcium silicate-coated paraffin/expanded perlite materials to improve the thermal performance of cement mortar," *Construction and Building Materials*, vol. 189, pp. 218–226, 2018.

[3] Y. Liu, M. Xie, E. Xu, X. Gao, Y. Yang, and H. Deng, "Development of calcium silicate-coated expanded clay based form-stable phase change materials for enhancing thermal and mechanical properties of cement-based composite," *Solar Energy*, vol. 174, pp. 24–34, 2018.

[4] Y. Liu, K. Yu, X. Gao, M. Ren, M. Jia, and Y. Yang, "Enhanced thermal properties of hydrate salt/poly (acrylate sodium) copolymer hydrogel as form-stable phase change material via incorporation of hydroxyl carbon nanotubes," *Solar Energy Materials and Solar Cells*, vol. 208, Article ID 110387, 2020.

[5] K. Yu, Y. Liu, F. Sun, M. Jia, and Y. Yang, "Graphene-modified hydrate salt/UV-curable resin form-stable phase change materials: continuously adjustable phase change temperature and ultrafast solar-to-thermal conversion," *Energy & Fuels*, vol. 33, no. 8, pp. 7634–7644, 2019.

[6] B. Lamrani, K. Johannes, and F. Kuznik, "Phase change materials integrated into building walls: an updated review," *Renewable and Sustainable Energy Reviews*, vol. 140, Article ID 110751, 2021.

[7] S. G. Yoon, Y. K. Yang, T. W. Kim, M. H. Chung, and J. C. Park, "Thermal performance test of a phase-change-material cool roof system by a scaled model," *Advances in Civil Engineering*, vol. 2018, Article ID 2646103, 2018.

[8] C. Fabiani, A. L. Pisello, A. D'Alessandro, F. Ubertini, L. F. Cabeza, and F. Cotana, "Effect of PCM on the hydration process of cement-based mixtures: a novel thermo-mechanical investigation," *Materials*, vol. 11, p. 871, 2018.

[9] A. Eddhahak-Ouni, S. Drissi, J. Colin, J. Neji, and S. Care, "Experimental and multi-scale analysis of the thermal properties of Portland cement concretes embedded with microencapsulated phase change materials (PCMs)," *Applied Thermal Engineering*, vol. 64, no. 1-2, pp. 32–39, 2014.

[10] A. L. Pisello, A. D'Alessandro, C. Fabiani et al., "Multifunctional analysis of innovative PCM-filled concretes," in *Proceedings of the 8th International Conference on Sustainability in Energy and Buildings*, R. Howlett, A. Capozzoli, and V. Serra, Eds., Seb-16, Turin, Italy, pp. 81–90, March 2017.

[11] D. P. Bentz and R. Turpin, "Potential applications of phase change materials in concrete technology," *Cement and Concrete Composites*, vol. 29, no. 7, pp. 527–532, 2007.

[12] H. Huang, X. Gao, K. H. Khayat, and A. Su, "Influence of fiber alignment and length on flexural properties of UHPC," *Construction and Building Materials*, vol. 290, Article ID 122863, 2021.

[13] H. Huang, X. Gao, and L. Teng, "Fiber alignment and its effect on mechanical properties of UHPC: an overview," *Construction and Building Materials*, vol. 296, Article ID 123741, 2021.

[14] H. Abbasi Hattan, M. Madhkhan, and A. Marani, "Thermal and mechanical properties of building external walls plastered with cement mortar incorporating shape-stabilized phase change materials (SSPCMs)," *Construction and Building Materials*, vol. 270, Article ID 121385, 2021.

[15] C. Guardia, G. Barluenga, I. Palomar, and G. Diarce, "Thermal enhanced cement-lime mortars with phase change materials (PCM), lightweight aggregate and cellulose fibers," *Construction and Building Materials*, vol. 221, pp. 586–594, 2019.

[16] T. Shi, W. Sun, and Y. Yang, "Preparation and heat storage/release behavior of latent heat storage gypsum-based building materials," *Materials and Structures*, vol. 47, no. 3, pp. 533–539, 2014.

[17] L.-C. Pop, M. Baibarac, I. Anghel, and L. Baia, "Gypsum composite boards incorporating phase change materials: a review," *Journal of Nanoscience and Nanotechnology*, vol. 21, no. 4, pp. 2269–2277, 2021.

[18] S. A. Memon, "Phase change materials integrated in building walls: a state of the art review," *Renewable and Sustainable Energy Reviews*, vol. 31, pp. 870–906, 2014.

[19] Y. Liu, M. Xie, X. Gao, Y. Yang, and Y. Sang, "Experimental exploration of incorporating form-stable hydrate salt phase change materials into cement mortar for thermal energy storage," *Applied Thermal Engineering*, vol. 140, pp. 112–119, 2018.

[20] X. Bao, H. Yang, X. Xu et al., "Development of a stable inorganic phase change material for thermal energy storage in buildings," *Solar Energy Materials and Solar Cells*, vol. 208, Article ID 110420, 2020.

[21] R. Ye, W. Lin, X. Fang, and Z. Zhang, "A numerical study of building integrated with CaCl2·6H2O/expanded graphite composite phase change material," *Applied Thermal Engineering*, vol. 126, pp. 480–488, 2017.

[22] G. Sang, Y. Zhang, M. Fan et al., "Thermo-mechanical properties of compaction molded cement-based composite containing a high mass fraction of phase change material for thermal energy storage," *Composites Part A: Applied Science and Manufacturing*, vol. 128, Article ID 105657, 2020.

[23] Y. He, X. Zhang, and Y. Zhang, "Preparation technology of phase change perlite and performance research of phase change and temperature control mortar," *Energy and Buildings*, vol. 85, pp. 506–514, 2014.

[24] D. Sun and L. Wang, "Utilization of paraffin/expanded perlite materials to improve mechanical and thermal properties of cement mortar," *Construction and Building Materials*, vol. 101, pp. 791–796, 2015.

[25] S. Ramakrishnan, X. Wang, J. Sanjayan, and J. Wilson, "Thermal performance assessment of phase change material integrated cementitious composites in buildings: experimental and numerical approach," *Applied Energy*, vol. 207, pp. 654–664, 2017.

[26] Z. Zhang, G. Shi, S. Wang, X. Fang, and X. Liu, "Thermal energy storage cement mortar containing n-octadecane/expanded graphite composite phase change material," *Renewable Energy*, vol. 50, pp. 670–675, 2013.

[27] B. Xu, H. Ma, Z. Lu, and Z. Li, "Paraffin/expanded vermiculite composite phase change material as aggregate for developing lightweight thermal energy storage cement-based composites," *Applied Energy*, vol. 160, pp. 358–367, 2015.

[28] A. Sharma, V. V. Tyagi, C. R. Chen, and D. Buddhi, "Review on thermal energy storage with phase change materials and applications," *Renewable and Sustainable Energy Reviews*, vol. 13, no. 2, pp. 318–345, 2009.

[29] K. Yu, Y. Liu, and Y. Yang, "Review on form-stable inorganic hydrated salt phase change materials: preparation, characterization and effect on the thermophysical properties," *Applied Energy*, vol. 292, Article ID 116845, 2021.

[30] Y. Liu, F. Sun, K. Yu, and Y. Yang, "Experimental and numerical research on development of synthetic heat storage form incorporating phase change materials to protect concrete in cold weather," *Renewable Energy*, vol. 149, pp. 1424–1433, 2020.

[31] A. D'Alessandro, A. L. Pisello, C. Fabiani, F. Ubertini, L. F. Cabeza, and F. Cotana, "Multifunctional smart concretes with novel phase change materials: mechanical and thermo-energy investigation," *Applied Energy*, vol. 212, pp. 1448–1461, 2018.

[32] H. Zhang, F. Xing, H.-Z. Cui et al., "A novel phase-change cement composite for thermal energy storage: fabrication, thermal and mechanical properties," *Applied Energy*, vol. 170, pp. 130–139, 2016.

[33] P.-H. Chen and D. D. L. Chung, "Mechanical energy dissipation using cement-based materials with admixtures," *ACI Materials Journal*, vol. 110, pp. 279–289, 2013.

[34] K. Yu, B. Jin, Y. Liu, and L. Li, "Enhanced thermal conductivity of form-stable phase change materials using carbon nanofiber-expanded graphite hybrid structure," *Materials Research Express*, vol. 6, no. 2, 2019.

[35] P. Yu, Z. Wang, P. Lai, P. Zhang, and J. Wang, "Evaluation of mechanic damping properties of montmorillonite/organo-modified montmorillonite-reinforced cement paste," *Construction and Building Materials*, vol. 203, pp. 356–365, 2019.

[36] B. Li, B. Huo, R. Cao, S. Wang, and Y. Zhang, "Sulfate resistance of steam cured ferronickel slag blended cement mortar," *Cement and Concrete Composites*, vol. 96, pp. 204–211, 2019.

[37] H. Zhao, Q. Xiao, D. Huang, and S. Zhang, "Influence of pore structure on compressive strength of cement mortar," *Science World Journal*, vol. 2014, Article ID 247058, 2014.

[38] M. Li and J. Shi, "Review on micropore grade inorganic porous medium based form stable composite phase change materials: preparation, performance improvement and effects on the properties of cement mortar," *Construction and Building Materials*, vol. 194, pp. 287–310, 2019.

[39] L. Liu and M. Eriten, "Frictional energy dissipation in wavy surfaces," *Journal of Applied Mechanics-Transactions of the Asme*, vol. 83, 2016.

[40] L. Chi, S. Lu, and Y. Yao, "Damping additives used in cement-matrix composites: a review," *Composites Part B: Engineering*, vol. 164, pp. 26–36, 2019.

[41] M. Li, Z. Wu, and J. Tan, "Heat storage properties of the cement mortar incorporated with composite phase change material," *Applied Energy*, vol. 103, pp. 393–399, 2013.

[42] X. Fang, Z. Zhang, and Z. Chen, "Study on preparation of montmorillonite-based composite phase change materials and their applications in thermal storage building materials," *Energy Conversion and Management*, vol. 49, no. 4, pp. 718–723, 2008.